

# Multicolour observations of V404 Cyg and J1118+480 with ULTRACAM

T. Shahbaz\*, V. Dhillon<sup>†</sup>, T.R. Marsh\*\*, C. Zurita<sup>‡</sup>, C. Haswell<sup>§</sup>, P.A. Charles\*\*, R.I. Hynes<sup>¶</sup> and J. Casares\*

*\*Instituto de Astrofísica de Canarias, 38200 La Laguna, Tenerife, Spain*

*†Department of Physics and Astronomy, University of Sheffield, Sheffield, S3 7RH, UK*

*\*\*Department of Physics and Astronomy, University of Southampton, Southampton, SO17 1BJ, UK*

*‡Observatorio Astronómico de Lisboa, Tapada da Ajuda 1349-018, Lisboa, Portugal*

*§Department of Physics and Astronomy, The Open University, Walton Hall, Milton Keynes, MK7 6AA, UK*

*¶Astronomy Department, The University of Texas at Austin, 1 University Station C1400, Austin, Texas 78712-0259, USA*

**Abstract.** We present high time-resolution multicolour observations of the quiescent soft X-ray transients V404 Cyg and XTEJ1118+480 obtained with ULTRACAM. The power density spectrum (PDS) of the V404 Cyg data shows a quasi-periodic oscillation (QPO) feature at 0.78 mHz ( $\approx 21.5$  min), whereas the PDS of the XTEJ1118+480 data shows a break. We discuss the possible origins for the QPO feature and break-frequency in the context of the advection-dominated accretion flow model.

## ULTRACAM

ULTRACAM is an ultra-fast, triple-beam CCD camera. The light is split into three wavelengths colours (blue, green and red) by two dichroic beamsplitters. The detectors are three back-illuminated, thinned, Marconi frame-transfer  $1024 \times 1024$  active area CCD chips with a pixel scale of 0.3 arcsecs/pixel. The CCDs are cooled using a three-stage peltier device and water chiller, resulting in negligible dark current. With the frame transfer mode, the dead-time is essentially zero (for further details see (Dhillon & Marsh 2001)).

## THE FLARES IN V404 CYG

ULTRACAM observations of V404 Cyg taken on the William Herschel Telescope (WHT, La Palma) during the period 2002 Sep 9 to 13 using the Sloan  $u'$ ,  $g'$  and  $i'$  filters with effective We used exposure times of 5.0 sec (“slow” data) and 0.237 sec (“fast” data).

Superimposed on the secondary star’s ellipsoidal modulation are large flares on timescales of a few hours, as well as several distinct rapid flares on timescales of tens of mins (see Figure 1). Although large amplitude flares are observed on more than one night, it is only on Sep 10 that a large flare is observed throughout the event. The shape of the large flares seem to be symmet-

ric with similar rise and decay times. Superimposed on these large flares are many rapid events which last typically  $\sim 0.5$  hr. Furthermore, superimposed on these flares, are still shorter term events on timescales of mins which show unresolved peaks. In general all the flare events appear to have a linear rise and decay and typically have a rise time of 2 mins and a duration of 6 mins (Shahbaz et al., 2003).

## THE POWER DENSITY SPECTRUM

We use the method of Lomb-Scargle to compute the PDS. The Lomb-Scargle method was chosen so that we could combine consecutive runs and confidently compute the periodogram. Also, in order to allow a direct comparison with X-ray PDS, we use the same normalisation method as is commonly used in X-ray astronomy, where the power is normalised to the fractional root mean amplitude squared per hertz. To compute the PDS we use the constraints imposed by the Nyquist frequency and the typical duration of each observation. We then average the PDS for each observing sequence. We bin and fit the PDS in logarithmic space and the errors in each bin are determined from the standard deviation of the points within each bin. The white noise level was subtracted by fitting the highest frequencies with a white noise plus red noise model.

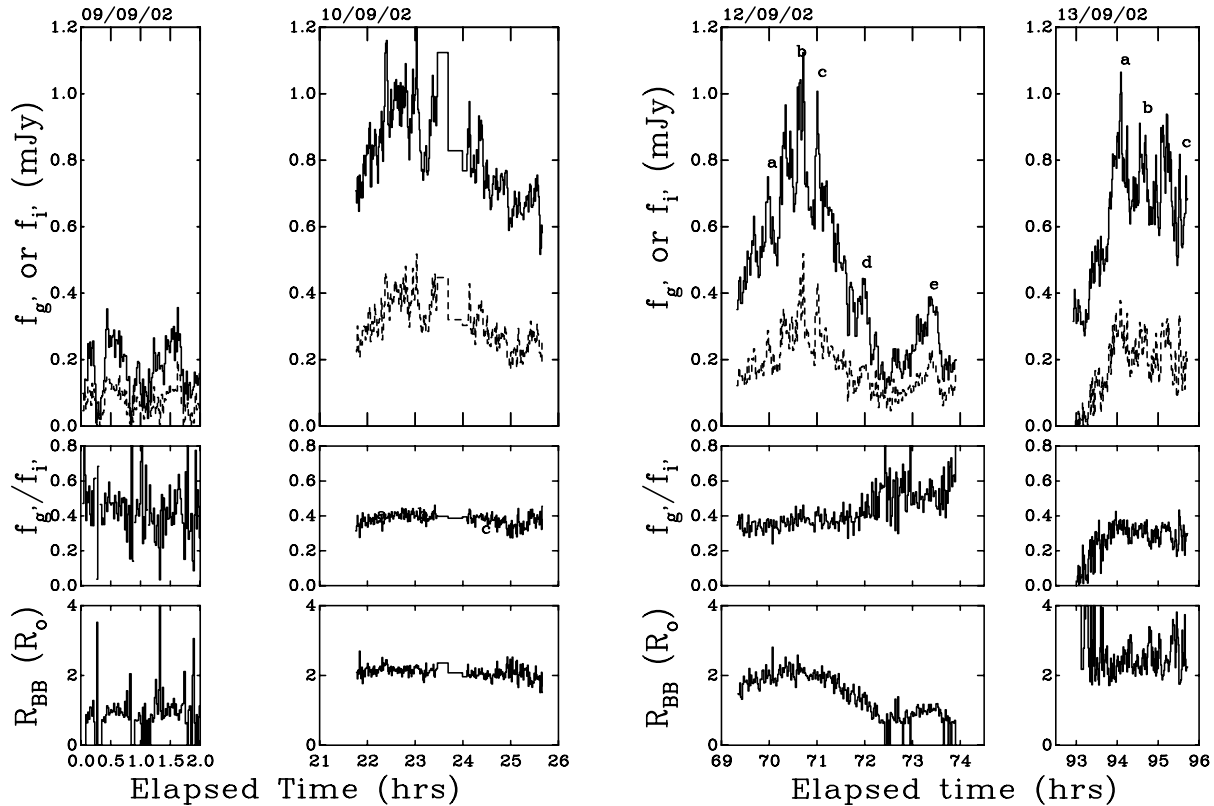


**FIGURE 1.** In the top panel we show the flare flux density lightcurve in the  $g'$  (dashed line) and  $i'$  (solid line) bands, obtained by subtracting the reddened secondary star’s ellipsoidal modulation from the observed lightcurves. For clarity the flare lightcurves have been re-binned to a time resolution 1 min. The uncertainties in the  $g'$  and  $i'$  lightcurves are 0.02 mJy and 0.01 mJy respectively. The middle panels show the flux density ratio  $f_{g'}/f_{i'}$  and the bottom panel shows the projected blackbody radius of the region producing the flares.

A QPO feature with a centroid frequency at 0.78 mHz ( $= 21.5$  mins) is present (see Figure 2), not surprising given that one can clearly see variability on timescales of 0.5-1.0hrs in the lightcurves. The fractional root mean squared amplitude is 3 and 1.3 percent for the  $g'$  and  $i'$  band QPOs and was computed by integrating the Gaussian function and taking the square root. The computed “fast”PDS has a power-law shape with a slope of  $-1.16 \pm 0.04$  ( $1-\sigma$  errors). As a check we also computed the PDS of the comparison star. Again the derived PDS was flat, which is exactly as expected for white noise data.

During the large flares the power-law index of the spectral energy distribution is  $\sim -2.0$  ( $F_\nu \propto \nu^\alpha$ ). It is difficult to explain this in terms of optically thin synchrotron emission, unless the electrons follow a much steeper power-law energy distribution ( $N(E)dE \propto E^p dE$ ). For solar and stellar flares the  $\alpha$  is  $\sim -0.5$ . The colour of the flares is consistent with optically thin gas with a temperature of  $\sim 8000$  K arising from a region with an equivalent

blackbody radius of at least  $2 R_\odot$ , which covers 3 percent of the accretion disc’s surface (Shahbaz et al., 2003).

### The QPO feature and the ADAF model

Interactions between the hot inner ADAF and the cool, outer thin disk, at or near the transition radius ( $r_{tr}$ ), can be a source of optical variability, due to synchrotron emission by the hot electrons in the ADAF. The variability could be quasi-periodic and would have a characteristic timescale given by a multiple of the Keplerian rotation period at  $r_{tr}$   $t_K \sim (M/10M_\odot)(r/100)^{1.5}$  s. If we assume that the 0.78 mHz QPO feature observed in the PDS is the dynamical timescale at the transition radius, then  $r_{tr}$  lies at  $10^{4.0} r_{sch}$ , which is consistent with other estimates (Narayan, Barret & McClintock 1997).

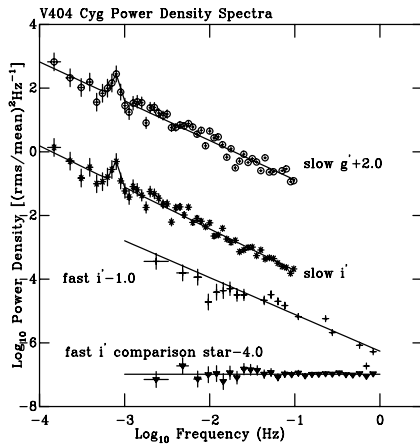


**FIGURE 2.** The PDS of V404 Cyg. From top to bottom: V404 Cyg  $g'$  and  $i'$  “slow” PDS, V404 Cyg  $i'$  “fast” PDS and the comparison star PDS.

## QUIESCENT J1118+480 VARIABILITY

ULTRACAM observations of J1118+480 taken in June 2003 on the WHT with exposure times of 11.6 sec (“slow” data) and 1.6 sec (“fast” data).

The low/Hard state X-ray PDS of J1118+480 shows a break at  $\sim 30$  Hz (Hynes et al., 2003). The quiescent optical PDS shows a break at  $\sim 1$  mHz (see Figure 3). Although the origin of the break is unknown, it is plausible that it scales with size of the inner region of the disc. Since the Low/Hard state has a higher X-ray luminosity than the quiescent state, and similarly involves an evaporated central region, and similarly involves an evaporated central region, the shift in the break frequency indicates that a larger evaporated region is present in quiescence.

## ACKNOWLEDGMENTS

TS acknowledges support from the Spanish Ministry of Science and Technology under project AYA 2002 03570. RIH is currently supported by NASA through Hubble Fellowship grant #HF-01150.01-A awarded by the Space Telescope Science Institute, which is operated by the Association of Universities for Research in Astronomy, Inc., for NASA, under contract NAS 5-26555. VSD and TRM acknowledge the support of PPARC through the grant PPA/G/S/1998/00534. Based on observations made with the William Herschel Telescope operated on the island of La Palma by the Isaac Newton Group in the Spanish Observatorio del Roque de los Muchachos of the Instituto de Astrofísica de Canarias.

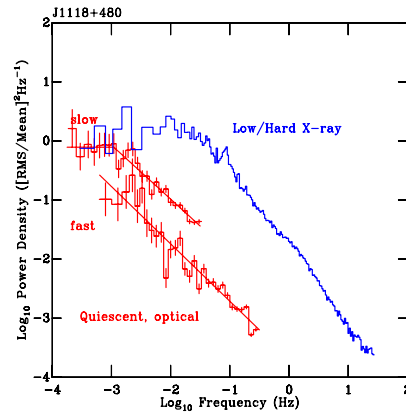


**FIGURE 3.** The quiescent optical PDS of XTE J1118+480 (left) and the Low/Hard state X-ray PDS (right) taken from Hynes et al., (2003). Note the shift in the break frequency.

## REFERENCES

1. Dhillon, V., and Marsh, T.R., 2001, *NewAR*, **45**, 91
2. Narayan R., Barret D., McClintock J.E., 1997, *ApJ*, **482**, 448
3. Hynes R.I., Haswell C.A., Cui W., Shrader C.R., O’Brien K., Chaty S., Skillman D.R., Patterson J., Horne K., 2003, *MNRAS*, **345**, 292
4. Shahbaz T., Dhillon V., Marsh T.R. Zurita C., Haswell C.A., Charles P.A., Hynes R.I., Casares J., 2003, *MNRAS*, **346**, 1116